REPORT SSD-TR-90-05

(4)

Single Event Upset in Irradiated 16K CMOS SRAMs

Prepared by

C. L. AXNESS, J. R. SCHWANK, P. S. WINOKUR,
J. S. BROWNING, and D. M. FLEETWOOD
Sandia National Laboratories
Albuquerque, NM 87185

and

R. KOGA
Space Sciences Laboratory
Laboratory Operations
The Aerospace Corporation
El Segundo, CA 90245

20 February 1990

Prepared for

SPACE SYSTEMS DIVISION
AIR FORCE SYSTEMS COMMAND
Los Angeles Air Force Base
P.O. Box 92960
Los Angeles, CA 90009-2960

This report was submitted by The Aerospace Corporation, El Segundo, CA 90245, under Contract No. F04701-85-C-0086-P00019 with the Space Systems Division, P.O. Box 92960, Los Angeles, CA 90009. It was reviewed and approved for The Aerospace Corporation by H. R. Rugge, Director, Space Sciences Laboratory. Lt Tyron Fisher was the project officer for the Mission-Oriented Investigation and Experimentation (MOIE) program.

This report has been reviewed by the Public Affairs Office (PAS) and is releasable to the National Technical Information Service (NTIS). At NTIS, it will be available to the general public, including foreign nationals.

This technical report has been reviewed and is approved for publication. Publication of this report does not constitute Air Force approval of the report's findings or conclusions. It is published only for the exchange and stimulation of ideas.

TYRON FISHER, LT, USAF
MOIE Project Officer
SSD/CLFPO

RAYMOND M. LEONG, MAJ, USAF
MOIE Program Manager
AFSTC/WCO OL-AB

UNCLASSIFIED

SECURITY CLASSIFICATION OF THIS PAGE

REPORT DOCUMENTATION PAGE

1a. REPORT SECURITY CLASSIFICATION Unclassified	1b. RESTRICTIVE MARKINGS
2a. SECURITY CLASSIFICATION AUTHORITY	3. DISTRIBUTION/AVAILABILITY OF REPORT Approved for public release; distribution unlimited.
2b. DECLASSIFICATION/DOWNGRADING SCHEDULE	
4. PERFORMING ORGANIZATION REPORT NUMBER(S) TR-0088(3940-05)-10	5. MONITORING ORGANIZATION REPORT NUMBER(S) SSD-TR-90-05
6a. NAME OF PERFORMING ORGANIZATION The Aerospace Corporation Laboratory Operations 6b. OFFICE SYMBOL (If applicable)	7a. NAME OF MONITORING ORGANIZATION Space Systems Division
6c. ADDRESS (City, State, and ZIP Code) El Segundo, CA 90245	7b. ADDRESS (City, State, and ZIP Code) Los Angeles Air Force Base Los Angeles, CA 90009-2960
8a. NAME OF FUNDING/SPONSORING ORGANIZATION 8b. OFFICE SYMBOL (If applicable)	9. PROCUREMENT INSTRUMENT IDENTIFICATION NUMBER F04701-85-C-0086-P00019
8c. ADDRESS (City, State, and ZIP Code)	10. SOURCE OF FUNDING NUMBERS PROGRAM ELEMENT NO. / PROJECT NO. / TASK NO. / WORK UNIT ACCESSION NO.

11. TITLE (Include Security Classification)
Single Event Upset in Irradiated 16K CMOS SRAMs

12. PERSONAL AUTHOR(S) Axness, C. L., Schwank, J. R., Winokur, P. S., Browning, J. S., Fleetwood, D. M. (Sandia National Laboratories); and Koga, R. (The Aerospace Corporation)

13a. TYPE OF REPORT	13b. TIME COVERED FROM _____ TO _____	14. DATE OF REPORT (Year, Month, Day)	15. PAGE COUNT
		1990 February 20	25

16. SUPPLEMENTARY NOTATION

17. COSATI CODES			18. SUBJECT TERMS (Continue on reverse if necessary and identify by block number)
FIELD	GROUP	SUB-GROUP	Single event upset tests Static RAMs

19. ABSTRACT (Continue on reverse if necessary and identify by block number)

The single-event upset (SEU) characteristics of a CMOS SRAM cell irradiated under conditions that simulate the total dose degradation anticipated in space applications are experimentally and theoretically investigated. Simulations of SEU sensitivity, utilizing a two-dimensional circuit/device simulator, with measured transistor threshold-voltage shifts and mobility degradations as inputs, are shown to be in good agreement with experimental data at high total dose. Both simulation and experiment show a strong SRAM-cell SEU "imbalance," resulting in a more SEU-tolerant "preferred" state and a less-tolerant "nonpreferred" state. The resulting cell imbalance causes an overall degradation in SEU immunity, which increases with increasing total dose and which should be taken into account in SEU testing and part characterization.

20. DISTRIBUTION/AVAILABILITY OF ABSTRACT	21. ABSTRACT SECURITY CLASSIFICATION	
☒ UNCLASSIFIED/UNLIMITED ☐ SAME AS RPT. ☐ DTIC USERS	Unclassified	
22a. NAME OF RESPONSIBLE INDIVIDUAL	22b. TELEPHONE (Include Area Code)	22c. OFFICE SYMBOL

DD FORM 1473, 84 MAR

83 APR edition may be used until exhausted.
All other editions are obsolete

SECURITY CLASSIFICATION OF THIS PAGE

UNCLASSIFIED

PREFACE

The authors would like to thank Ken Gutierrez, Ken Hughes, Danny Turpin, and Steve Rodgers for their help in irradiating integrated circuits (ICs) and transistors. We also thank Ron Jones and Henry White for providing ICs and test transistors. We are indebted to the staffs at the Lawrence Berkeley Laboratory (LBL) 88–in. cyclotron and the Brookhaven Tandem van de Graaf for their assistance in providing beam for single-event upset (SEU) experiments. The help of personnel at The Aerospace Corporation was greatly appreciated in taking data at LBL. We are also indebted to Gerard Simmons for building and adjusting the Sandia SEU test chamber at Brookhaven National Laboratory. Finally, the first author wishes to thank Paul Dressendorfer and Fred Sexton of Sandia National Laboratories for their technical discussions and comments during the writing of this report.

CONTENTS

FIGURES

TABLES

1. INTRODUCTION

Space satellite systems are simultaneously exposed to ionizing radiation and high-energy cosmic ions. Ionizing radiation induces changes in the electrical characteristics of metal-oxide semiconductor devices, such as the threshold voltage and mobility, which are bias- and total-dose dependent [1,2]. High-energy ions, on the other hand, may cause single-event upsets (SEU) in the static random-access memories (SRAMs) [3]. The SEU sensitivity of a SRAM, in turn, depends on transistor drive and timing, which are dependent on threshold-voltage shifts and mobility degradations. It follows, therefore, that the SEU sensitivity of a SRAM in space should depend on the dose it receives in space.

Since most of the work described in this report depends on the "state" of the SRAM, we introduce some terminology. We say a SRAM is in the "0" state if the data-in line is held at VSS volts and all addresses are written (as a "0"). We say the SRAM is in the "1" state if the data-in line is held at VDD and all addresses are written (as a "1"). A 0/1 irradiation and anneal simply means that the SRAM was irradiated in the "0" state and annealed in the "1" state. All of our experiments are 0/1 irradiation/anneals. Finally, we note that the "0" and "1" state in general have different SEU characteristics because the n- and p-channel transistors in the cell are irradiated under different biases for different states. The cross section for the "0" state is the cross section measured when the SRAM is in the "0" state. We also use the notation $0 \rightarrow 1$, referring to cells switching from the "0" state to the "1" state during SEU testing, for this cross section. The "1" state cross section and $1 \rightarrow 0$ are synonymous in this work. A cross section is said to be "saturated" when it is equal to the total sensitive area of the chip for the mechanism causing SEU. For our complementary metal-oxide semiconductor (CMOS) technology and the feedback resistances reported here, this is always the sum of the areas of the off p-channel transistor drains and depletion regions (approximately 4×10^{-2} cm^2). A "preferred" state exists when it has a higher critical LET [L_c, the LET (linear energy transfer) at which 10^{-2} cm^2 cross section is measured] for SEU than the opposite state. Since in all cases the 0×1 cross section had a higher critical LET than the $1 \rightarrow 0$ cross section, the preferred state is synonymous with the irradiated or "0" state in this work.

Experimental results [2] indicate that ionizing radiation induces bias-dependent transistor threshold-voltage shifts (ΔV_{th}) and mobility degradations, which cause a SRAM cell imbalance. SRAM cell imbalance is defined as the difference between n-channel threshold shifts [2]. An alternative definition of cell imbalance is the difference in n-channel transistor drives after irradiation, which takes into account bias-dependent mobility degradation as well as threshold shifts. We are concerned with the n-channel transistor drives because on our SRAM the most sensitive strike location is the off p-channel drain, which is restored through an n-channel transistor. The cell imbalance results in one state of the SRAM being preferred over the other because of differences in n-channel drives for the "0" and "1" states.

Recent SEU experiments using low LET proton irradiations on commercial N-channel metal-oxide semiconductor (NMOS) SRAMs [4] show an increasing SEU cross section with dose in the nonpreferred state. In other recent SEU experiments [5] using a high-LET Cf-252 SEU source on low-dose irradiated CMOS SRAMs, no change in SEU cross section is observed after irradiation. However, the authors note that the source LET was sufficiently high so as to saturate the SEU-sensitive area of the part [5]. Although the findings of [4] and [5] appear to conflict, they may easily be explained by examining the cross section in the nonpreferred state over a wider range of LET and noting that, within one range of LET, the cross section increases with dose; whereas, within another range, the cross section remains constant.

The purpose of this work is to investigate the state dependence of SEU on total dose over a wide range of LET at both high-dose-rate Co-60 irradiations and low-dose-rate Cs-137 irradiations. In addition, we compare the predicted SEU response from our two-dimensional (2D) transient circuit/device simulator using experimentally measured transistor threshold-voltage shifts and mobility degradations as input to experimentally measured SEU degradation in irradiated ICs. Finally, we investigate the dependence of SEU immunity on total dose.

2. EXPERIMENTAL DETAILS AND MODELING

We performed a series of experiments on a large number of CMOS SRAMs with variable feedback resistances, using both high-dose-rate Co-60 and low-dose-rate Cs-137 sources for irradiation, and with various high-energy ions offering a range of LETs for SEU testing. These experiments give a clearer picture of the effect of cell imbalance on SEU characteristics and show that total dose degrades overall SEU immunity since the nonpreferred state becomes softer after irradiation. Finally, we compare experiments with results obtained using a 2D circuit/device simulator in which experimentally determined bias-dependent transistor threshold-voltage shifts and mobility degradations are input parameters.

The test vehicles used for experiment in this study were the CMOS 16k SA3240 SRAMs fabricated at Sandia National Laboratories. Feedback resistors (R_f) [3] harden the cell against SEU by slowing the transfer of transient signals between the right- and left-hand inverters constituting the cell. Production SA3240 SRAMs have 400-k Ω feedback resistors and do not experience SEU at any experimentally available LET. In order to get measurable SEU cross sections, the tested memories were obtained from a lot in which the feedback resistance was below specification, and as such, SEU results in this report are not representative of Sandia production parts. The SA3240 has a 2-μm channel length and a 320-Å-thick gate oxide.

An advanced 2D transient finite difference device/circuit code [6] was used to simulate SEU in irradiated SRAMs. Figure 1 illustrates the irradiated CMOS SRAM cell as simulated. Nodes N1 and N2 represent the information nodes of the cell. An ion strike is depicted at the off p-channel drain. The decoupling (feedback) resistors, R_f, slow transient signals between the inverters formed by transistors P1/N1 and P2/N2. Simulations were carried out in a manner similar to that detailed in previous nonirradiated SRAM cell publications [7], except that the code was modified to accept transistor-dependent mobility degradations, and voltage offsets were introduced at the gate of each transistor to simulate threshold-voltage shifts. For simulations of a Co-60 irradiated SRAM cell, threshold-voltage shifts and mobility degradations were determined from irradiated test transistors from the same lot as the tested ICs. For simulations of a low-dose-rate Cs-137 irradiated cell, threshold-voltage shifts and mobility degradations were taken from available data from a different SA3240 lot [8]. These data are compiled in Table 1.

Within the off p-channel drain area, there is a spatial dependence of SEU on LET. In order to define the sensitive SEU area for a single cell, simulations were performed at the most sensitive drain location (the center of the drain) [9], as well as the least sensitive location (the drain edge). Subsequent simulations were made, adjusting the strike LET with a constant multiplier until the LETs just initiating SEU at these drain locations were found. Simulation showed that the onset of SEU at the drain edge occurred at approximately 5 MeV-cm^2/mg higher LET than at the drain center. This information was used in the construction of simulated cross section vs LET curves.

Table 1. Threshold Shifts (ΔV_{th}) and Mobility Degradations (μ/μ_o) from Test Transistors After a 150-krad Co-60 Irradiation at a Fixed Bias Followed by an 80-hr Anneal in the Opposite Bias, and a 500-krad Cs-137 Low-Dose-Rate Irradiation. The dose rate for the 150-krad(Si) irradiation was 233 rad(Si)/s, and the rate for the 500-krad(Si) irradiation was 0.23 rad(Si)/s.

Total Dose, krad	P-off		P-on		N-off		N-on	
	ΔV_{th}	μ/μ_o	ΔV_{th}	μ/μ_o	ΔV_{th}	μ/μ_o	ΔV_{th}	μ/μ_o
150	-0.50	0.87	-0.14	0.96	0.63	0.87	-0.15	0.87
500	-0.92	0.83	-0.28	0.95	0.16	0.71	0.23	0.71

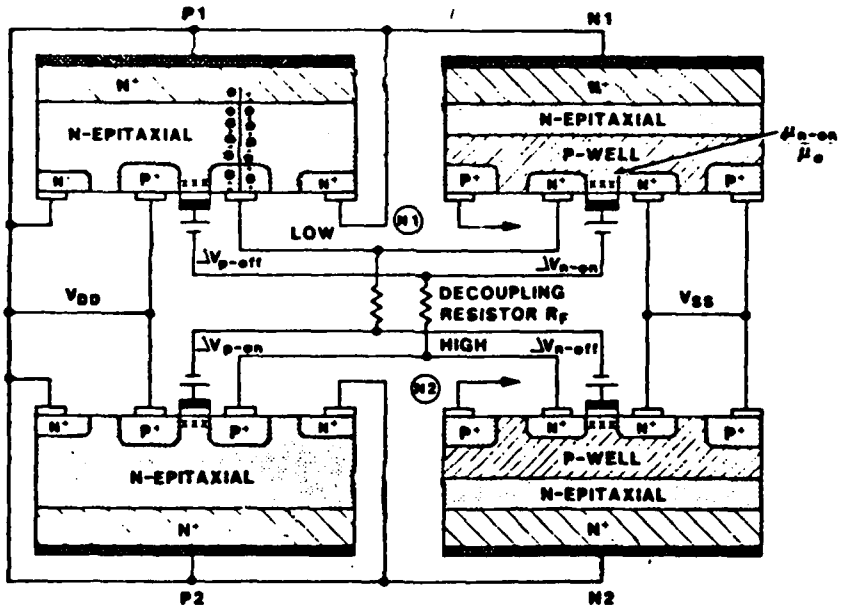

Fig. 1. Circuit Diagram of a Simulated Irradiated SRAM Cell Without Access Transistors. Decoupling resistors (R_f) protect against SEU by slowing the transfer of transient pulses between the inverters composing the cell. Bias-dependent mobility degradations and voltage offsets model total dose effects. An ion strike is depicted at the off p-channel drain.

3. INITIAL EXPERIMENT

An initial experiment was performed to verify if SEU degradation and a preferred state for a SRAM exist after irradiation. In this case, four parts were irradiated in the "0" state to 500 krad(Si) at a dose rate of 160 rad(Si)/s with a Shepherd Co-60 source [1]. The irradiation was followed by a 5-day 100°C anneal in the "1" state. One part was left nonirradiated as a control. The procedure of irradiation followed by a high-temperature anneal is currently used to simulate a space-satellite environment [10]. Irradiating and annealing in opposite SRAM states is currently thought to give the worst-case SRAM imbalance in terms of threshold-voltage shifts and mobility degradations [2].

SEU testing of these parts was carried out at the Brookhaven National Laboratory Tandem Van de Graaf in a manner similar to th· · 'escribed previously [11], using a custom design test chamber. The chamber is equipped with four pin diodes located approximately 1/2 cm above, below, and to each side of the beam centerline to ensure good beam alignment. A scintillator foil and photomultiplier tube were used as a counter. The ions used in the test were 333-MeV Au, 261-MeV I, 279-MeV Br, and 97-MeV Cl, which provide normal incidence LETs of 77, 58, 38, and 12 MeV-cm^2/mg, respectively. These ions provide effective LETs in the range of 12-144 MeV-cm^2/mg by adjusting the beam angle of incidence [11].

The results of this experiment are compiled in Table 2. To examine the results, we compare the postirradiation-critical LET for a part with preirradiation-critical LETs measured in the past SEU experiments [12] for a part with the same feedback resistor. We note that the critical LET for the nonirradiated part #2263 agrees well with these previous SEU data. The first point to be made from these data is that the parts with feedback resistors (R_f) less than 190 kΩ show a large shift in critical LET (at least 50 MeV-cm^2/mg) when postirradiation data are compared with typical SA3240 preirradiation data [12]. In addition, comparison of the postirradiation L_c for the two SEU-tested cell states shows that the SRAM prefers the state it was irradiated in. Finally, we note that the two parts with large feedback resistances (2260 and 2254) did not experience sufficient total dose degradation to experience SEU, even after bombardment by 60-deg incident 333-MeV Au ions with LETs of 154 MeV-cm^2/mg.

Table 2. Results of SEU Tests on Irradiated SRAMs for the Initial Experiment. L_c is defined to be the LET in MeV-cm^2/mg at which the cross section is 10^{-5} cm^2. The parts were irradiated in a Co-60 Shepherd cell to 500 krad(Si) in the "0" state followed by a 5-day 100°C anneal in the"1" state. Dose enhancement effects are not considered in the total dose calculation.

Part Number	R_f, kΩ	Total Dose, krad	Dose Rate, rad/s	Pre-rad L_c	Post-rad L_c (1→0)	Post-rad L_c (0→1)
2270	154	500	160	72*	22	35
2263	160	---	---	78	--	--
2265	186	500	160	120*	< 36‡	> 154†
2260	262	500	160	> 154*	154†	> 154†
2254	370	500	160	> 154*	154†	> 154†

*These pre-rad values were estimated from past SA3240 data (see Ref. 11).

†Cross section measured less than 10^{-5} cm^2 at this LET.

‡Cross section measured greater than 10^{-5} cm^2 at this LET.

4. HIGH-DOSE-RATE EXPERIMENT

A. IRRADIATIONS

A second set of experiments was performed on a larger number of parts to analyze the effect of various Co–60 total doses on SEU immunity. In these experiments, all parts were SEU tested in their preirradiated condition at the Lawrence Berkeley Laboratory (LBL) cyclotron. All devices were then irradiated at Sandia using either a Shepherd or gamma cell in the "0" state and annealed 1 day (one set of parts was annealed 5 days) in the "1" state at 80°C. Total dose irradiations of 150, 200, 300, and 500 krad(Si) were carried out. After irradiation and anneal, the devices were returned to the LBL facility for SEU testing. Some parts were irradiated, annealed, and SEU tested twice with a 30–day period between irradiations.

Table 3 gives a partial compilation of the results of this testing. Note the same general behavior in this data set as in the initial experiment. In addition, the trend of the data shows that the difference between preirradiation and postirradiation L_c increases with total dose, indicating a degradation of SEU immunity with total dose. In particular, parts that are irradiated twice always show increased SEU degradation with total dose. Finally, we see that for the "0" state ($0 \rightarrow 1$), L_c is higher and hence the part is harder after a low (less than 300 krad(Si)) total dose irradiation; whereas at higher total dose, the "0" state is generally softer (L_c lower) than at preirradiation.

Figure 2 gives the measured cross section vs LET for a part that was Co–60 irradiated to 150 krad(Si) at a dose rate of 230 rad(Si)/s in the "0" state followed by a 5–day 80°C anneal in the "1" state. Both the preferred ($0 \rightarrow 1$ in figure) and nonpreferred ($1 \rightarrow 0$ in figure) states are shown, as well as the preferred state after a second 150–krad(Si) 0/1 irradiation/anneal. In addition, the preirradiation–measured cross section vs LET for the part is shown. In the preirradiated condition the cell is balanced, and both the "0" ($0 \rightarrow 1$) and "1" ($1 \rightarrow 0$) cross sections are the same. The leftward shift of the $1 \rightarrow 0$ cross section vs LET curves indicates that the part gets softer with increasing total dose. The cross–section curve for $0 \rightarrow 1$ SEU is to the right of the $1 \rightarrow 0$ cross–section curve, establishing the "0" state as the preferred state. In this case, the preferred state hardened after irradiation.

B. SIMULATIONS

SEU in a SRAM cell with 144–kΩ feedback resistors was simulated using threshold shifts and mobility degradations measured on test transistors that had experienced 150–krad(Si) Co–60 irradiations in either off or on bias and an 80–hr 80°C anneal in the opposite bias. The sensitive SEU area of the cell was found as per the discussion at the end of section 2. The radiation/anneal conditions and cell parameters are approximately the same as those experienced by the IC tested in the previous section. The simulated cross section vs LET curve is shown in Fig 3.

Table 3. Partial Results of SEU Tests on Irradiated SRAMs for High-Dose-Rate Experiments. L_c is defined to be the LET in MeV-cm^2/mg at which the cross section is 10^{-5} cm^2. Irradiations are carried out in either a Shepherd or gamma cell. Anneals are either 1 or 5 days in the "1" state at 80°C. Dose-enhancement effects are not considered in the total dose calculation.

Part Number	R_f, kΩ	Total Dose, krad	Dose Rate, rad/s	Pre-rad L_c	Post-rad L_c (1→0)	Post-rad L_c (0→1)
9545	144	150	233	43	39	48
9566	182	150	233	>76†	65	>76†
9550	194	150	233	>76†	>76†	
9572	196	200	233	>76†	45	
9545*	144	300	233	43	<30‡	
9550*	194	300	233	>76†	45	
9548	156	500	233	57	17	27
9551	182	500	233	>76†	21	27
9569	184	500	233	>76†	19	

*These parts were irradiated twice. Second irradiation performed after a 30-day period.
†Cross section measured less than 10^{-5} cm^2 at this LET.
‡Cross section measured greater than 10^{-5} cm^2 at this LET.

There is good qualitative agreement between the simulated data in Fig. 3 and the experimental data in Fig. 2. Both exhibit a leftward shift of the cross section vs LET curve when the part is in the "1" state, i.e., 1 → 0 transistions. Both show the 0 → 1 cross sections vs LET curve to the right of the preirradiation cross section, indicating a hardening of the "0" state. However, the simulated preirradiation L_c was approximately 20 MeV-cm^2/mg greater than the experimental L_c, and the postirradiation shift in L_c was much greater in simulation than in experiment.

C. DISCUSSION

In Fig. 2 the preirradiation cross section appears to be converging to a value less than the sum of the off p-channel transistor drains (4×10^{-3} cm^2), as would be expected in a SA3240 SRAM with 144-kΩ feedback resistance. We speculate that this behavior is due to variations in either the cell feedback resistance or the drive of the n-channel transistors, which restore the cell after a single event by sinking charge collected at the off p-channel transistor drains [7]. This variation is for cells of a

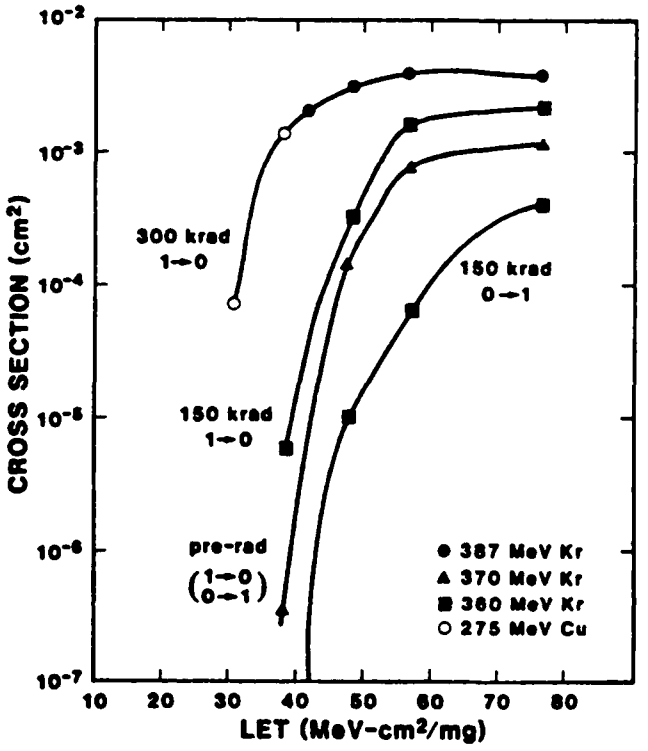

Fig. 2. Experimental Cross Section as a Function of LET for Preirradiation, After a 150-krad(Si) Co-60 Irradiation, and After a Second 150-krad(Si) Co-60 Irradiation. Both irradiations were performed in the "0" state followed by a 1-5 day 80°C anneal in the "1" state. The second irradiation occurred after a 30-day period. The cross section for both the preferred ("0") state and the nonpreferred ("1") state are shown for the first 150-krad(Si) irradiation/anneal.

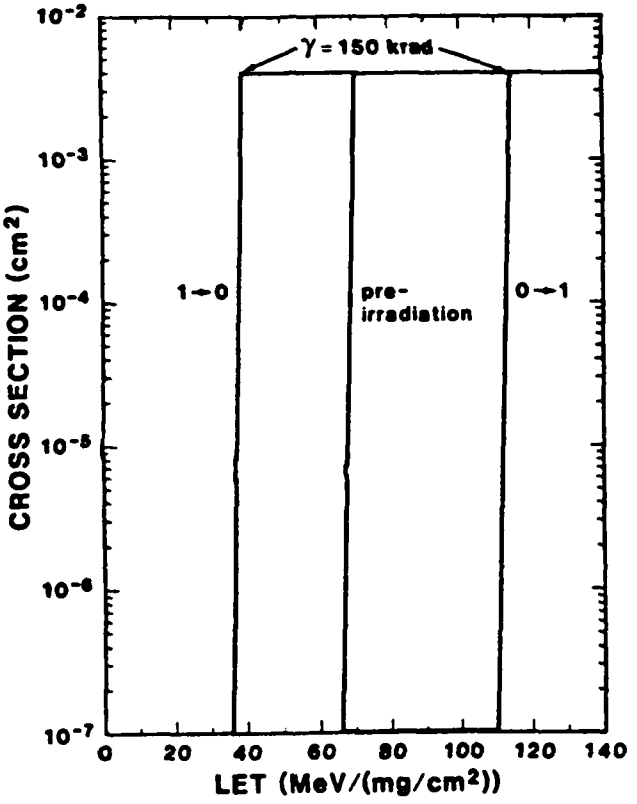

Fig. 3. Simulated Cross Section as a Function of LET for Preirradiated and Postirradiated SA3240 SRAM with 144 kΩ Feedback Resistors. Threshold-voltage shifts and mobility degradations are taken from test transistors irradiated to 150 krad(Si) by a Co–60 source in the "0" state followed by a 1-day 80°C anneal in the "1" state. All 16k cells are assumed to have the same SEU characteristics as the single simulated cell in this construction. Postirradiation preferred ("0") and nonpreferred ("1") states are shown.

single SRAM chip. The slope of the cross section vs LET curve near L_c was not as steep as typically seen, also possibly indicating a spread in drive or feedback resistance within the chip. In addition, a few parts in this experiment had preirradiation L_c that did not correlate well with the feedback resistance measured on the test structure of the chip that is used to characterize the feedback resistance for the part. This also indicates possible variation of feedback resistance in the chip and may explain why the simulated L_c is somewhat higher than the experimental L_c in Figs. 2 and 3. It is intuitively obvious that the tightness in the distribution of feedback resistance or n-channel transistor drive directly affects the shape of the cross-section curves, suggesting that SEU data can be used as a tool in assessing cell drive/feedback resistor variability. Variability of feedback resistance in the tested parts will not qualitatively affect the results of these experiments, since individual cells will harden or soften only as a function of dose, dose rate, and cell state during irradiation/anneal. Speculation on the variability of feedback resistance and transistor parameters applies only to this low-feedback-resistance lot and not to normal Sandia production lots.

Finally, we note that the shift in critical LET is quantitatively greater in simulation than in experiment for the 150-krad data shown. We note that the experimental data presented are for an IC that did not experience a very large shift in L_c compared with other ICs irradiated to 150 krad(Si). The on n-channel threshold-voltage shift in the transistor data, on the other hand, was the same as that seen in previous 200-krad(Si) Co-60 irradiations [2]; so it is not unreasonable for the simulations to predict a shift on the order of 30 MeV-cm^2/mg. The simulations do a good job of qualitatively modeling the direction of the L_c shifts.

5. LOW-DOSE-RATE EXPERIMENT

A. IRRADIATIONS

A final experiment was carried out to see the effect of a low-dose-rate irradiation [0.23 rad(Si)/s] on SRAM SEU characteristics. This lower dose rate is closer to the dose rate seen in space, although still a few orders of magnitude higher. The experiment was performed in a Cs-137 Shepherd cell. In order to reduce dose-enhancement effects, the parts were placed inside a lead-aluminum box within the cell in a procedure described in [1]. All parts were irradiated to 500 krad(Si) at 0.23 rad(Si)/s in the "0" state. No high-temperature anneal was necessary at this dose rate. Parts were SEU tested before and after irradiation at the LBL cyclotron at Berkeley.

Table 4 gives a partial compilation of the results from this experiment. The experimentally observed preirradiation to postirradiation shift in critical LET is approximately 20–30 MeV-cm^2/mg. Figure 4 shows the experimentally measured section vs LET curve for a part with 162-kΩ feedback resistors that was irradiated to 500 krad(Si) at a dose rate of 0.23 rad/s by a Cs-137 source. We note that again the "1" state SEU cross section ($1 \rightarrow 0$) shifts to the left of the preirradiation cross section. At this higher total dose, however, the "0" state cross section ($0 \rightarrow 1$) also shifts to the left of the preirradiation cross section, although not as far as the "1" state. This behavior was also seen with high-dose-rate Co-60 irradiations to 300 krad(Si) or greater. We note that since the $0 \rightarrow 1$ cross section did not shift as far to the left as the $1 \rightarrow 0$ cross section, the "0" state is again the preferred state.

Table 4. Partial Results of SEU Tests on Irradiated SRAMs for Low-Dose-Rate Experiments. L_c is defined to be the LET in MeV-cm^2/mg. Dose enhancement effects are not considered in the total dose calculation, but they are reduced by a Pb-Al shield.

Part Number	R_f, kΩ	Total Dose, krad	Dose Rate, rad/s	Pre-rad L_c	Post-rad L_c (1→0)	Post-rad L_c (0→1)
9546	150	500	0.23	47	30	
9544	162	500	0.23	57	30	39
9554	179	500	0.23	>76*	44	

*Cross section measured less than 10^{-5} cm^2 at this LET.

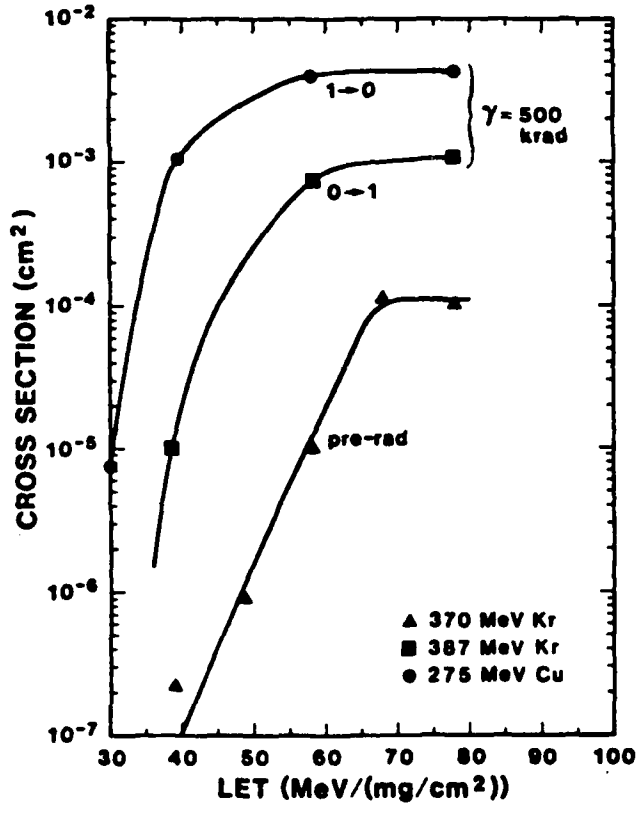

Fig. 4. Experimental Cross Section as a Function of LET for a Preirradiated and Postirradiated SA3240 SRAM with 162-kΩ Feedback Resistors. The part was irradiated to 500 krad(Si) at 0.23 rad(Si)/s by a Cs-137 source in the "0" state. The cross sections for both the preferred ("0") state and the nonpreferred ("1") state are shown.

B. SIMULATIONS

SEU in a SRAM with 160-kΩ feedback resistors was simulated using threshold-voltage shifts and mobility degradations measured on test transistors irradiated to 500 krad(Si) at 0.23 rad(Si)/s in a Shepherd Cs-137 cell. The threshold-voltage shifts and mobility degradations used in the simulations are shown in Table 1. Minimal LETs for the preirradiated cell and the postirradiation cell in the "0" and "1" states were calculated as prescribed at the end of section 2. A cross section vs LET curve was constructed assuming all 16k cells had the simulated SEU characteristics. Figure 5 shows this simulated cross section vs LET curve.

C. DISCUSSION

In this case, we have good qualitative and quantitative agreement between simulation and experiment. Both the $0 \rightarrow 1$ and $1 \rightarrow 0$ postirradiation cross sections shift to the left of the preirradiation cross section vs LET curve. The amount of the shift is in good agreement, being 27 MeV-cm^2/mg both in experiment and simulation for the $1 \rightarrow 0$ cross section. For the $0 \rightarrow 1$ cross section, the shifts in L_c are 12 MeV-cm^2/mg (in simulation) and 18 MeV-cm^2/mg (in experiment). The experimental preirradiation L_c remains somewhat lower than the simulated value. However, it must be noted that the slope of the experimental cross-section curve in the nonsaturated region is not steep. If it were more vertical, the agreement between experimental and simulated L_c would be good. We also note that the preirradiation and $0 \rightarrow 1$ cross sections approach a value less than full p-drain saturation at high LET. We believe the reason for this is the variability in feedback resistance or transistor drive discussed previously (see discussion in section 4).

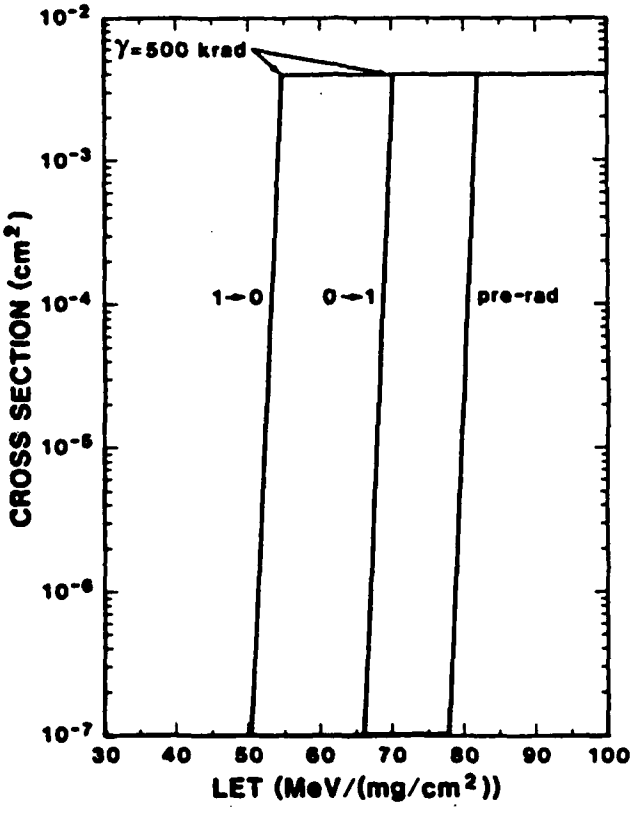

Fig. 5. Simulated Cross Section as a Function of LET for a Preirradiated and Postirradiated SA3240 SRAM with 160-kΩ Feedback Resistors. Threshold-voltage shifts and mobility degradations are taken from test transistors irradiated to 500 krad(Si) at 0.23 rad(Si)/s by a Cs-137 source in the "0" state. All 16k cells are assumed to have the same SEU characteristics as the single simulated cell in this construction. Postirradiation preferred ("0") and nonpreferred ("1") states are shown.

6. GENERAL DISCUSSION

Parts irradiated to 150 and 200 krads(Si) in Table 3 show very little shift in critical LET. The present feedback-resistor specification for the SA3240 is 400 kΩ. The parts with 262-kΩ and 370-kΩ feedback resistances did not experience any SEU, even after a 500-krad(Si) Co-60 irradiation. Parts with lower feedback resistances did, however, show significant degradation in their critical LET at high doses (greater than 300 krad(Si)). We conclude that, for up to 200 krad(Si) total dose at room temperature, SEU degradation resulting from total dose is not significant. Further study should be conducted to characterize SEU in irradiated SA3240s at high temperatures.

From Fig. 3, it is easy to explain the apparent discrepancy between the increasing cross section at low-ion LET and the constant cross section at high-ion LET in [4] and [5], respectively. The authors of [5] postulate that the difference was due to a shift in L_c, which is seen as an increase in cross section at low LET but as a constant saturated cross section at high LET. Although the SA3240 illustrated is more SEU immune than the parts used in [4] and [5], this behavior is demonstrated in Fig. 3 by considering tests conducted at LETs of 40 and 75 MeV-cm^2/mg. Subsequent irradiations and SEU testing in the "1" state will show an increasing cross section for the LET = 40 MeV-cm^2/mg source and no change in cross section for the LET = 75 MeV-cm^2/mg source.

Finally, it is easy to see the reason why the preferred-state cross-section curve for the 150-krad(Si) total-dose exposure shifted right from the preirradiation cross section curve; while the 500-krad(Si) total-dose-exposure cross-section curve shifted left from a simple consideration of transistor threshold shifts. Note that when the SRAM is in its preferred state, an ion strike at the off p-channel drain restores itself through the n-channel transistor that was irradiated at on bias. Examination of Table 1 indicates that after the 150-krad(Si) irradiation, the on n-channel threshold shift is negative, increasing the drive of the transistor, which, in turn, causes the struck node to recover faster. We therefore would expect the preferred state to become harder as was observed in simulation and experiment. On the other hand, the 500-krad(Si) on n-channel threshold shift is positive, reducing the transistor drive, which increases the struck node recovery time. Although the other threshold shifts and mobility degradations tend to slow the switching time of the cell, tending to harden it, in this case the increase in recovery time is the dominant effect and the preferred state becomes softer after irradiation, as shown in simulation and experiment.

7. CONCLUSIONS

We have shown that both low-dose-rate Cs-137 irradiation and high-dose-rate Co-60 irradiation cause a degradation of SEU immunity in CMOS SRAMs. This degradation of SEU immunity increases with increasing dose. At low total dose, up to 200 krad(Si), this degradation does not appear to be too great, at least at room temperature, where these experiments were conducted. At higher total dose, 500 krad(Si), degradation of SEU immunity is very significant for parts with feedback resistors in the range of 100-200 kΩ, but was not evident in the two SEU-tested parts that had high feedback resistance.

We showed that bias-dependent transistor threshold shifts and mobility degradations manifest themselves by imbalancing the SRAM, causing a preferred SEU state. This effect was demonstrated in both simulation and experiment.

REFERENCES

1. P. S. Winokur, F. W. Sexton, J. R. Schwank, D. M. Fleetwood, P. V. Dressendorfer, T. F. Wrobel, and D. C. Turpin, *IEEE Trans. Nucl. Sci.* **NS-33**, 1343 (1986); P. S. Winokur, F. W. Sexton, G. L. Hash, and D. C. Turpin, NS-34, 1448 (1987).

2. D. M. Fleetwood, P. V. Dressendorfer, and D. C. Turpin, *IEEE Trans. Nucl. Sci.* **NS-34**, 1178 (1987); D. M. Fleetwood and P. V. Dressendorfer, **NS-34**, 1408 (1987).

3. T. M. Mnich, S. E. Diehl, B. D. Shafer, R. Koga, W. A. Kolasinski, and A. Ochoa, Jr., *IEEE Trans. Nucl. Sci.* **NS-30**, 4620 (1983).

4. B. L. Bhuva, R. L. Johnson Jr., R. S. Gyurcsik, K. W. Fernald, and S. E. Kerns, *IEEE Trans. Nucl. Sci.* **NS-34**, 1414 (1987).

5. T. K. Sanderson, D. Mapper, J. H. Stephen, and J. Farren, *IEEE Trans. Nucl. Sci.* **NS-34**, 1287 (1987).

6. M. S. Mock, *Proc. of NASECODE III Conference*, Dublin, Ireland, 1911 (1983).

7. C. L. Axness, H. T. Weaver, J. S. Fu, R. Koga, and W. A. Kolasinski, *IEEE Trans. Nucl. Sci.* **NS-33**, 1577 (1986).

8. J. R. Schwank, F. W. Sexton, D. M. Fleetwood, R. V. Jones, R. S. Flores, M. S. Rodgers, and K. L. Hughes, *IEEE Trans. Nucl. Sci.* **NS-35** (6) (1988).

9. C. L. Axness, H. T. Weaver, and J. S. Fu, *Proc. of the NASECODE IV Conference*, J. J. H. Miller, ed., Boole Press, Dublin, Ireland (1985).

10. J. R. Schwank, P. S. Winokur, P. J. McWhorter, F. W. Secton, P. V. Dressendorfer, and D. C. Turpin, *IEEE Trans. Nucl. Sci. NS-31*, 1434 (1984).

11. R. Koga, and W. A. Kolasinski, *IEEE Trans. Nucl. Sci.* **NS-31**, 1190 (1984).

12. H. T. Weaver, C. L. Axness, J. D. McBrayer, J. S. Browning, J. S. Fu, A. Ochoa Jr., and R. Koga, *IEEE Trans. Nucl. Sci.* **NS-34**, 1281 (1986).

LABORATORY OPERATIONS

The Aerospace Corporation functions as an "architect-engineer" for national security projects, specializing in advanced military space systems. Providing research support, the corporation's Laboratory Operations conducts experimental and theoretical investigations that focus on the application of scientific and technical advances to such systems. Vital to the success of these investigations is the technical staff's wide-ranging expertise and its ability to stay current with new developments. This expertise is enhanced by a research program aimed at dealing with the many problems associated with rapidly evolving space systems. Contributing their capabilities to the research effort are these individual laboratories:

Aerophysics Laboratory: Launch vehicle and reentry fluid mechanics, heat transfer and flight dynamics; chemical and electric propulsion, propellant chemistry, chemical dynamics, environmental chemistry, trace detection; spacecraft structural mechanics, contamination, thermal and structural control; high temperature thermomechanics, gas kinetics and radiation; cw and pulsed chemical and excimer laser development, including chemical kinetics, spectroscopy, optical resonators, beam control, atmospheric propagation, laser effects and countermeasures.

Chemistry and Physics Laboratory: Atmospheric chemical reactions, atmospheric optics, light scattering, state-specific chemical reactions and radiative signatures of missile plumes, sensor out-of-field-of-view rejection, applied laser spectroscopy, laser chemistry, laser optoelectronics, solar cell physics, battery electrochemistry, space vacuum and radiation effects on materials, lubrication and surface phenomena, thermionic emission, photosensitive materials and detectors, atomic frequency standards, and environmental chemistry.

Electronics Research Laboratory: Microelectronics, solid-state device physics, compound semiconductors, radiation hardening; electro-optics, quantum electronics, solid-state lasers, optical propagation and communications; microwave semiconductor devices, microwave/millimeter wave measurements, diagnostics and radiometry, microwave/millimeter wave thermionic devices; atomic time and frequency standards; antennas, rf systems, electromagnetic propagation phenomena, space communication systems.

Materials Sciences Laboratory: Development of new materials: metals, alloys, ceramics, polymers and their composites, and new forms of carbon; nondestructive evaluation, component failure analysis and reliability; fracture mechanics and stress corrosion; analysis and evaluation of materials at cryogenic and elevated temperatures as well as in space and enemy-induced environments.

Space Sciences Laboratory: Magnetospheric, auroral and cosmic ray physics, wave-particle interactions, magnetospheric plasma waves; atmospheric and ionospheric physics, density and composition of the upper atmosphere, remote sensing using atmospheric radiation; solar physics, infrared astronomy, infrared signature analysis; effects of solar activity, magnetic storms and nuclear explosions on the earth's atmosphere, ionosphere and magnetosphere; effects of electromagnetic and particulate radiations on space systems; space instrumentation.